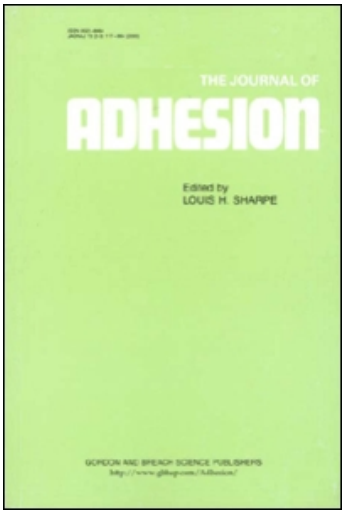

The Journal of Adhesion
Publication details, including instructions for authors and subscription information:
http://www.informaworld.com/smpp/title~content=t713453635

Scanning Electron Microscopic Studies on the Failure of Rubber-to-Metal Bonded Composites

Jossit Kurian[a]; G. B. Nando[a]; S. K. De[a]
[a] Rubber Technology Centre, Indian Institute of Technology, Kharagpur, India

To cite this Article Kurian, Jossit , Nando, G. B. and De, S. K.(1987) 'Scanning Electron Microscopic Studies on the Failure of Rubber-to-Metal Bonded Composites', The Journal of Adhesion, 20: 4, 293 — 316
To link to this Article: DOI: 10.1080/00218468708074949
URL: http://dx.doi.org/10.1080/00218468708074949

J. Adhesion, 1987, Vol. 20, pp. 293–316
Photocopying permitted by license only

Printed in the United Kingdom

Scanning Electron Microscopic Studies on the Failure of Rubber-to-Metal Bonded Composites

JOSSIT KURIAN, G. B. NANDO and S. K. DE

Rubber Technology Centre, Indian Institute of Technology, Kharagpur 721302, India

(Received March 4, 1986; in final form August 15, 1986)

Scanning electron microscopic studies were conducted to evaluate the failure mechanism of rubber-to-metal bonded composites in the 90° peel test (ASTM D 429-B). It was found that when cohesive failure in rubber takes place, the composites, failing by stick-slip mode, show high peel strength. Moreover, in such cases, there exists a linear correlation between the peel strength and the crosslink density of the rubber vulcanizate.

KEY WORDS electron microscopy; peel strength; cohesive failure; stick-slip failure; crosslink density; dewetting.

INTRODUCTION

Elastomers can be bonded to metals by a number of techniques, the most popular being the brass bonding[1] and the use of a proprietary bonding agent. An adhesive in its applications may encompass a wide range of elastomers and metals. One problem encountered in studying rubber-to-metal adhesion arises from the choice of a suitable test procedure, reproducible and above all capable of giving reliable data on the mode and energy of rupture rather than on the deformation of the adherends. By the existing conventional test methods, it is almost impossible to measure the true bond strength of strong adhesives because of the least chance of an interfacial failure.

The popular test methods for adhesion strength measurement are (a) direct tension test (butt joint test), (b) cone test and (c) peel test. The cone test, introduced by Painter[2] claimed to be a method of provoking interfacial failure between rubber and adhesive. But it was found[3] that, for strongly bonded systems, a thin layer of rubber was always sticking to the cone surface after failure showing cohesive nature of failure in rubber. It was shown that butt joint specimens have more chances of provoking rubber failure.[4] For quality control tests the peel test is popular because of the ease of test specimen preparation and the reproducibility. Peel testing is widely used to assess the performance of pressure sensitive tapes[5] where the type of failure may be either interfacial, either at the substrate or backing or cohesive failure of the adhesive. There are two approaches to the interpretation of peel tests—one by analysing the stresses set up in the adhesive layer on peeling and the other by using the energy conservation concept. It was reported that the former was highly impossible for nonlinear elastic materials and the latter was promising.[6]

For the surface characterisation and morphology studies of failed composites, scanning electron microscope (SEM) coupled with energy dispersive X-ray analyser was used by earlier workers.[7,8] In this paper, an attempt has been made to explain the peeling mechanism of the rubber-to-metal bonded systems in the 90° peel test by analysing the peeled surface using SEM and comparing the results with peel strength.

EXPERIMENTAL

Rubber-to-metal bonded composites were made by vulcanizing the rubber strip over the adhesive coated metal surface. The adhesive used was Chemlok 205 (primer) and Chemlok 220 (cover coat), supplied by M/s Hughson Chemicals, Lord Corporation, U.S.A.

1 Preparation of the rubber compound

Nine different compounds were prepared by varying the vulcanization system, filler type and loading with natural rubber as the base

TABLE I
Rubber compound formulations

Ingredient/ Compound no	A	B	C	D	E	F	G	H	I
Natural rubber[a]	100	100	100	100	100	100	100	100	100
Zinc oxide	5	5	5	5	5	5	5	—	5
Stearic acid	1.5	1.5	1.5	1.5	1.5	1.5	1.5	—	1.5
Sulfur	2.5	2.5	2.5	2.5	0.4	2.5	2.5	—	2.5
Dicumyl peroxide	—	—	—	—	—	—	—	3	—
CBS[b]	0.8	0.8	0.8	0.8	5	1	1.2	—	0.8
Silica[c]	—	—	—	—	—	25	40	—	—
Carbon black[d]	—	10	25	40	40	—	—	40	—
Hard clay	—	—	—	—	—	—	—	—	40
Process oil[e]	—	—	2	4	4	2	4	4	2
Antioxidant[f]	1.5	1.5	1.5	1.5	1.5	1.5	1.5	1.5	1.5
Diethylene glycol	—	—	—	—	—	2	2	—	—

[a] Grade ISNR-5.
[b] N-cyclohexyl 2-benzothiazole sulfenamide.
[c] Vulcasil-S.
[d] Grade N-330.
[e] Elasto 740 (aromatic type).
[f] Vulkanox HS.

polymer. The mixes were prepared on a laboratory size two roll mixing mill as per ASTM D 3184-80. The compounds were sheeted out and laid on clean cellophane paper to avoid contamination of the rubber surface. The cellophane was removed just before moulding. Formulation of the rubber compounds are given in Table I. Compounds containing three different vulcanization systems, namely, conventional system (that is, formulations A, B, C, D, F, G, I), efficient system (that is, formulation E) and peroxide system (that is, formulation H) were chosen in the present studies.

2 Preparation of the metal surface

The metal used was C-40 Steel (Indian Standards) in the form of rectangular strips of size $60.5 \times 25 \times 2$ mm. The strips were surface ground and cleaned using sand paper (40 grade). The metal surface

was cleaned with trichloroethylene and kept in desiccator not more than 15 minutes when it was coated with the adhesive system. The adhesive was coated on an area of 6.25 cm^2 with a brush while the rest of the area was covered by adhesive tape. Fifteen minutes after the application of the primer coat, the cover coat was applied and it was left for 30 minutes drying in a dust free chamber.

3 Preparation of the composites

The mould used was a two piece compartment mould with six rectangular cavities for compression moulding six specimens at a time.

Rubber blanks were prepared from the compounded sheet by cutting rectangular sheets out of it along the grain direction in order to eliminate grain effect among samples and to fit into the mould cavities. Rubber thickness in the composite was 6.4 mm. The vulcanization was done by using a single day-light, electrically-heated hydraulic press at 150°C and at a pressure of 650 psi to the respective optimum cure times as determined by the Monsanto Rheometer (R-100). The optimum cure times as measured from the rheographs (Figures 1a and 1b) of different rubber compounds are as follows: A, 8.9 min., B, 8.6 min., C, 8.3 min., D, 8.0 min., E, 13.1 min., F, 9.6 min., G, 10.5 min., H, 25.0 min., I, 11.9 min. The vulcanized samples were cooled at ambient temperature and tested after 24 hours.

4 Determination of peel strength of the composite

The peel strength was determined in accordance with ASTM D 429 method B using an Instron Universal Testing Machine (model 1195). Peeling was done at an angle 90° to the bonded surface. The test specimen was fitted horizontally in the special type of jaw to the upper grip of the Instron with the separating edge of the test sample towards the operator. The rubber tab was held by the movable lower grip of the machine. (The test sample and test method are shown in Figure 2a and 2b.) A steady load was applied at the rate of

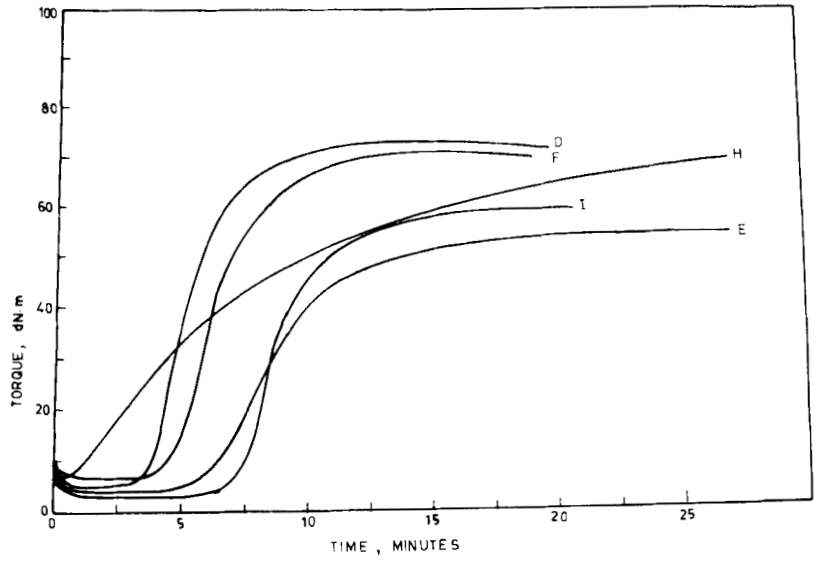

(a)

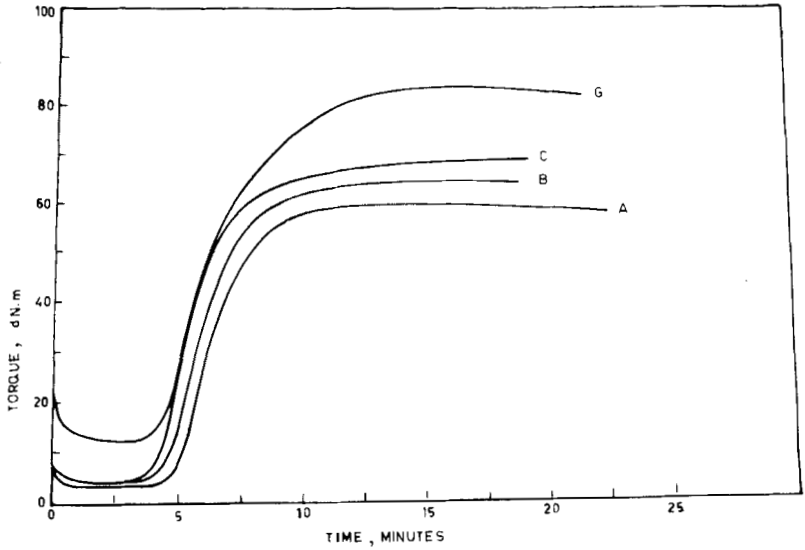

(b)

FIGURE 1(a) and (b) Rheograph of the rubber compounds at 150°C.

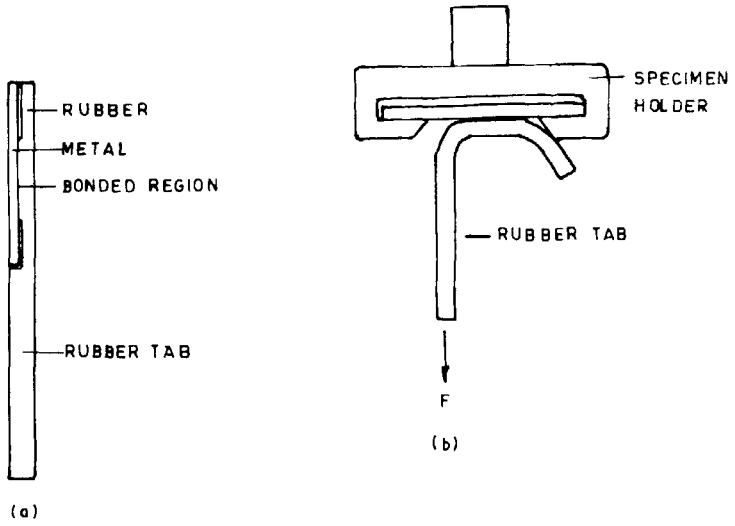

FIGURE 2(a) and (b) Rubber-to-metal bonded composite and the test assembly.

50 mm/min. until separation is complete. The peel force was recorded and expressed as kN/m, given in Table II.

5 Physical testing of the samples

Tensile strength of the mixes was determined at 25°C as per ASTM D-412-51T at a crosshead speed of 500 mm/min. using the Instron machine. Tear strength of the compounds was determined according to ASTM D-624-81 using the unnicked 90° angle test specimens (Die C) at the same crosshead speed as above. Hardness of the samples was determined by IRHD testing method. The test results are given in Table III.

6 Determination of crosslink density

The crosslink density of the vulcanizates was determined by swelling method using Mullins relationship.[9]

$$C_1 = (\rho RT(2M_c \text{ Chem})^{-1} + 0.78 \times 10^6) \times (1 - 2.3(M_c \text{ Chem})\, \bar{M}_n^{-1}) \text{ dynes/cm}^2$$

TABLE II
90° Peel strength of the composites

Compound no	Peel strength Max (kN/m)	Peel strength Min (kN/m)	Standard deviation of maxima	Standard deviation of minima	Mode of failure (visual)
A	—	—	—	—	No peeling occurred. Tab broken.
B	—	—	—	—	No peel, tab broken before peeling.
C	12.97	11.21	2.68	1.73	Cohesive failure in rubber. Stick-slip pattern on failure surface.
D	15.58	12.79	2.34	0.93	Cohesive failure in rubber as before. Number of stick lines less than before.
E	10.68	8.97	1.82	1.25	Cohesive failure in rubber. The wavy stick lines are not as prominent as previous samples.
F	14.35	—	—	—	Intermittent rubber and adhesive failure as indicated by black spots on failed metal surfaces.
G	18.35	—	—	—	Cohesive rubber failure and interfacial failure between rubber and adhesive; and cohesive failure of adhesive also visible.
H	4.44	—	—	—	Very smooth failure surface with fine wavy pattern.
I	7.59	—	—	—	Cohesive failure in rubber, smooth failure surface.
D_1†	13.47	10.79	2.50	1.40	Cohesive failure in rubber, stick-slip pattern visible.
D_2†	14.24	12.09	3.26	1.51	Cohesive failure in rubber, stick slip pattern visible.

† D_1, D_2, rubber compound D, but vulcanized for 5 minutes and 20 minutes respectively.

TABLE III
Physical properties of the rubber vulcanizates

Compound no	Hardness (IRHD)	Tensile strength (MPa)	Tear strength (kN/m)	Elongation at break (%)
A	47	23.24	33.80	875
B	47	25.87	33.29	720
C	54	32.03	60.49	671
D	61	31.60	80.67	602
E	60	22.34	69.58	558
F	60	34.80	60.05	921
G	72	29.84	75.52	825
H	54	16.65	48.00	365
I	53	26.22	32.78	781
D_1	56	29.87	81.81	638
D_2	65	26.71	81.35	525

and C_1 was calculated using the relation[10]

$$-\ln(1 - V_{r_0}) + V_{r_0} + \mu V_{r_0}^2 = 2C_1 V_s (V_{r_0}^{1/3} - V_{r_0}/2)/RT$$

where,

V_{r_0} = volume fraction of rubber network in the swollen gel, corrected for the effect of the filler using the equation derived by Porter,[11]
μ = Flory-Huggins solvent-rubber interaction parameter,
V_s = molar volume of the swelling liquid,
C_1 = elastic constant pertinent to the rubber hydrocarbon in the vulcanizate,
ρ = rubber vulcanizate density,
R = molar gas constant,
T = absolute temperature,
$\bar{M}_n$ = initial molecular weight of the rubber hydrocarbon in the compound,
$(2M_c \text{ Chem})^{-1}$ = density of chemical crosslinks expressed as mmol/kg of rubber hydrocarbon.

7 Scanning electron microscopy

Peeled metal as well as rubber surfaces were sputter-coated with gold within 24 h of peeling and studied under Philips 500 model scanning electron microscope at 33° tilt.

RESULTS AND DISCUSSION

A rubber-to-metal bonded composite on peeling gives two fractured surfaces one containing the metal part of the composite and the second, the rubber part of the composite as shown in Figure 3. In the studies conducted, these surfaces were examined by SEM.

Stick-slip failure phenomena

Some rubber compounds bonded to metal, while peeling, fail in a special mode leaving a thin layer of rubber on the metal surface in the 90° peel test. Both the rubber and metal surface have the so called stick lines and slip regions alternatively. This is characterised by the typical shape of the force-separation curve as shown in Figure 4. The initial increase in force up to the point 'A' is accompanied by very slow peeling giving a thin, rough failure pattern. This is followed by a catastrophic rubber failure and the force relaxes to a minimum value. As the lower grip of the machine continues to move, the stress at the peel front again increases. With the naked eye it can be observed that a very slow peeling takes place at the peel front during this time. Since the rate of

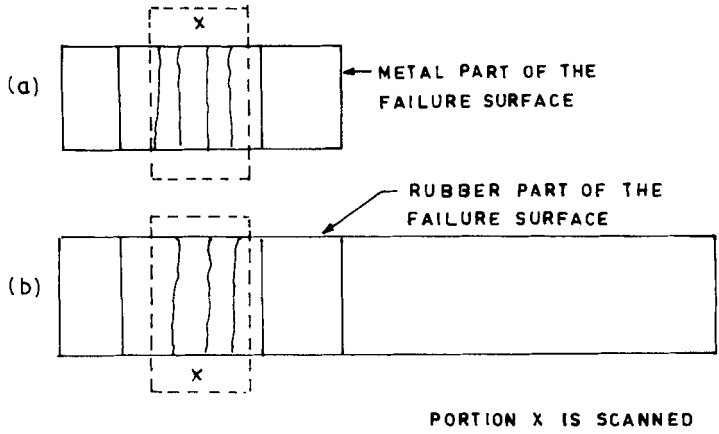

FIGURE 3(a) and (b) Composite failure surfaces by peeling. Portions shown inside discontinuous line was scanned.

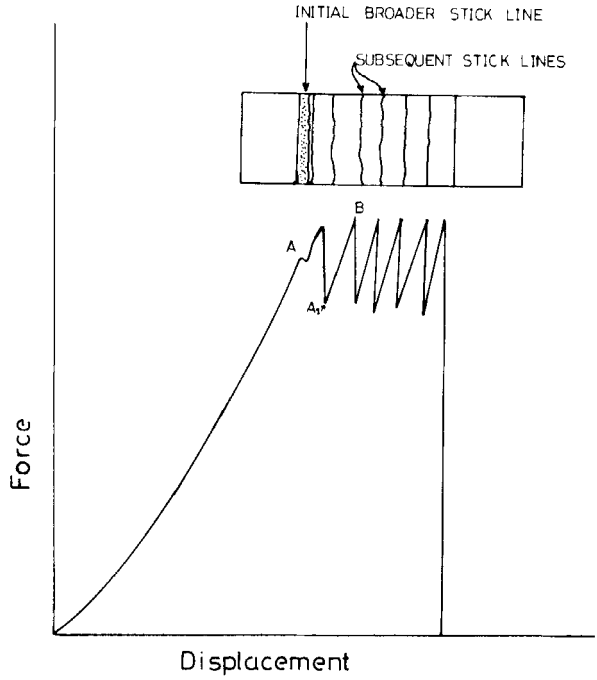

FIGURE 4 Force-separation curve of the composite along with the failure surface.

propagation of this slow peeling is lower compared to the development of stress at the peel front, this stress continues to increase until it reaches a particular value B, then catastrophic failure results. This process repeats until the rubber is fully separated from the metal. This mode of failure is called stick-slip failure.

The rubber compounds C, D, E, D_1 and D_2 exhibit the stick-slip failure pattern, leaving a thin layer of rubber on the metal surface. It was found by examining the failure surface that the first stick region is the broadest and the subsequent ones are line-like. This may be due to the viscoelastic property of the rubber since the duration of action of force in the first stick region will always be higher. The time taken to reach the failure force of the first stick region and the average for the rest of the stick lines as measured from the force-separation curves is given in Table IV.

TABLE IV
Duration of action of forces on the composites

Compound no	Width of 1st stick region (cm)	Time taken to reach the max of force in 1st stick region, t_0 (sec)	Time taken to reach max force in subsequent stick regions t_1 (sec)	Force variation during the period t_1 (kN/m)	Force increase by t_0
C	0.233	108	16.0	11.23 to 12.97	0 to 10.81
D	0.156	105	23.4	12.75 to 15.58	0 to 14.14
E	0.346	78	9.4	8.97 to 10.68	0 to 9.25
D_1	0.233	108	16.0	10.79 to 13.47	0 to 10.90
D_2	0.133	66	11.2	12.10 to 14.24	0 to 11.17

It was found that as the maximum force developed in a stick region increases, the subsequent slip width becomes higher. There is almost a linear relationship between the slip width and the force developed at the stick region as shown in Figure 5. When this curve is extrapolated to zero slip width, a particular force value is obtained that can peel the sample without the stick-slip pattern (Table V).

When the failed rubber surface was elongated it was found that the stick regions which appeared as lines (Figure 4) were actually made of cracks as shown in Figure 6. This can be explained as follows. During the course of peeling, the peel front was in a highly strained state in the stick region. A slow peeling occurred in this region as the force there continued to increase due to the downward movement of the crosshead of testing machine. This resulted in removing material towards the metal surface from the rubber forming a comparatively long shallow depression on the rubber failure surface. Before each catastrophic failure, this phenomenon occurred. As soon as the rubber was fully separated from the metal, it regained its original size due to elastic recovery forming the so called cracks.

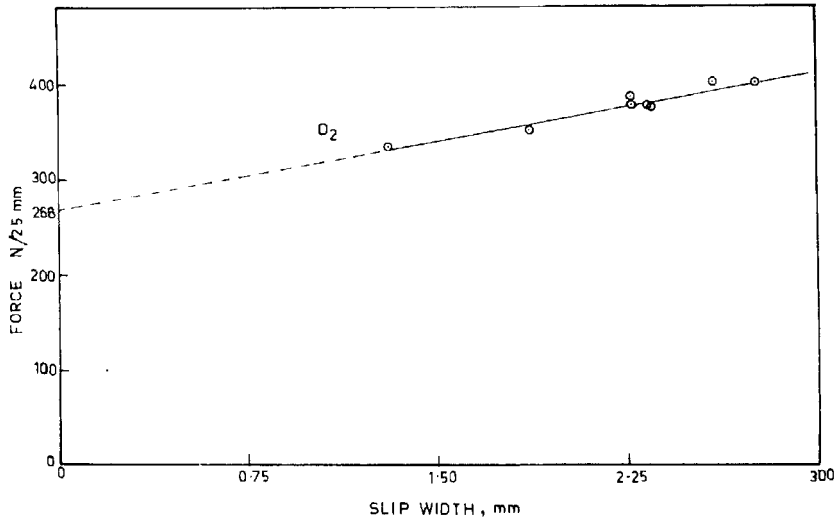

FIGURE 5 Graph showing linear relation between slip width and the force developed to cause slip (Typical example—compound D_2).

The rate of peel propagation in the stick region is so slow that the force relaxation occurring by this process is very small compared to the increase of force due to the downward movement of the rubber tab. Hence, excess force concentration occurs at the peel front and, when this reaches a particular value, a sudden breakage of peel front occurs, resulting in a catastrophic failure of rubber. This may be the reason for stick-slip failure.

It was found that the standard deviation of the peak values of force-separation curve was greater than that of the minima values as

TABLE V
Force/25 mm for zero slip width

Sl no	Compound no	Force (N)
1	C	252.15
2	D	379.88
3	E	215.87
4	D_1	243.13
5	D_2	268.00

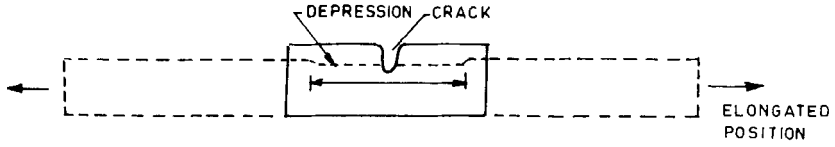

FIGURE 6 Figure explaining the crack formation on rubber surface due to peeling.

given in Table II. During stick-slip mode of failure cohesive failure in rubber was taking place and hence the peel strength would be related to the physical properties of the rubber. Due to the higher non-uniformity of the peak force values, taking an average of these values as peel strength is questionable. On the other hand, standard deviation of the minima force values were much less than that of peak values and we also observed a very good linear relationship with the crosslink density of rubber and average minima force value (Figure 7). Hence, these minima values which were just sufficient to propagate catastrophic failure in rubber are more relvant in the design of the rubber compound than the maxima values.

Compounds H & I have lower peel strength and show smooth failure surface as compared to formulations C, D and E having stick-slip failure. Therefore it can be inferred that when the cohesive failure in rubber is taking place, compounds having stick-slip failure have higher peel strength.

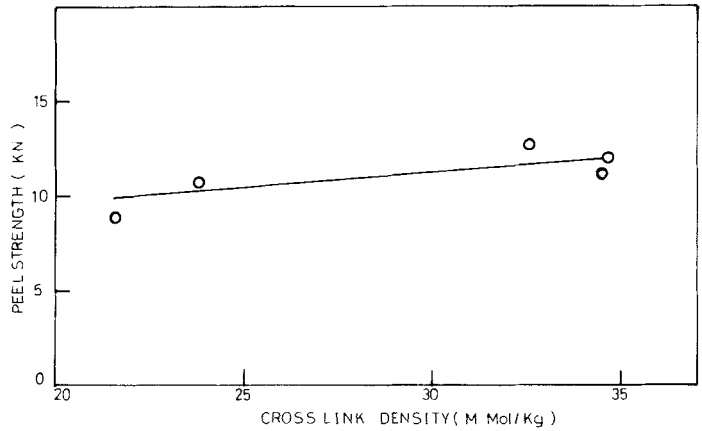

FIGURE 7 Crosslink density *vs* minimum peel strength of carbon black filled vulcanizates.

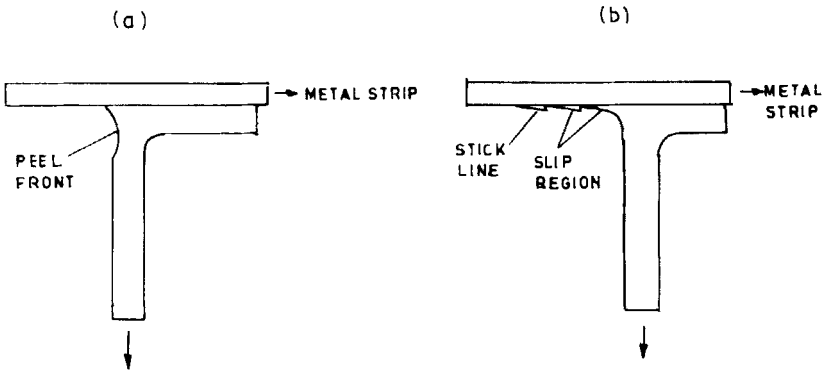

FIGURE 8(a) and (b) Geometry of the peel front at the start and intermediate period of peel.

It was reported[7] that the first stick region is closer to the adhesive surface than the subsequent regions. As shown in Figure 8 (a and b) the virgin peel front is in direct contact with the adhesive and once peel has started, the peel front will be a part of the previous arrested peel front. Hence, the peel strength in the first peak of the force separation curve will have more significance than the rest of the peaks in connection with adhesion strength.

SEM observations

Figures 9 and 10 are the fractographs showing the fracture surfaces of metallic part and rubber part, respectively, of the peeled surfaces of compound D bonded to the metal. The stick line and slip region are clearly seen. The cracks that appear on either of the photographs continue breadthwise end to the end. These cracks correspond to the stick region. A crack on the rubber part of the failure surface is expected to coincide with a ridge on the rubber surface which is sticking to the metal surface after failure (Figure 3). But we observed a crack instead of a ridge (Figure 9), possibly due to the occurrence of the slow peeling at a highly strained peel front and the subsequent catastrophic failure through a comparatively less strained rubber. This ridge is seen as given in Figure 12.

Figure 11 shows the slip area and flow channels that emanate

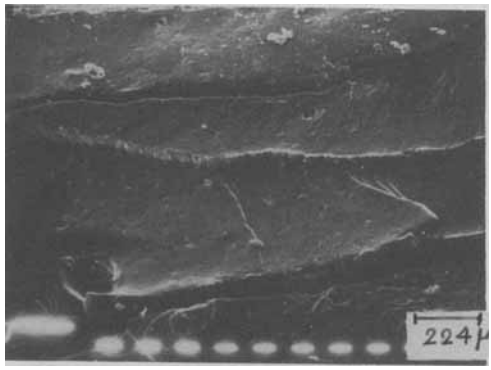

FIGURE 9 SEM photograph of compound D showing the peeled metal surface (50×).

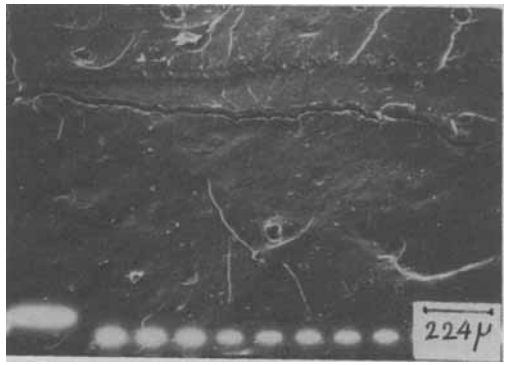

FIGURE 10 SEM photograph of compound D showing the peeled rubber surface (50×).

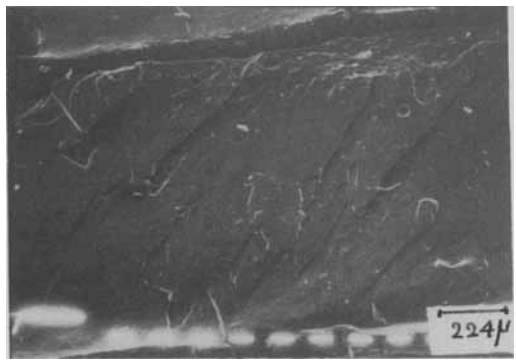

FIGURE 11 Photomicrograph of compound D showing the slip region after peeling (50×).

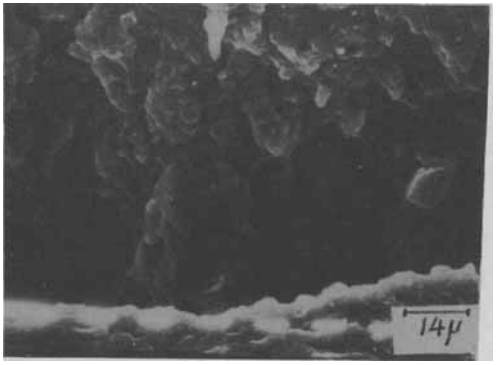

FIGURE 12 Photomicrograph showing the inside of a crack of compound D (800×).

from a crack while the peeling was in progress. These channels show the direction of peel of the bulk rubber from the metal. A magnified view of the inside of a crack (Figure 12, referred in the previous paragraph) on the metal part of the fractured surface, shows the dimpled structure of the rubber inside indicating the slow peeling that has occurred. It is characteristic of ductile failure of rubber,[12] corresponding to the region A_1 to B in the force-displacement diagram (Figure 4).

If the metal part of the failed composite is immersed in benzene the thin film of rubber swells and separates from the metal surface. A second film which was still sticking on the metal surface swells only very slowly and is obviously the adhesive. Thus, from the qualitative point of view, the differential swelling of the two thin substrates corresponds to that of the rubber and adhesive. Similar phenomena were observed in the case of compounds D_1, D_2 and C bonded to metal.

From the above observations, it is evident that cohesive failure of rubber took place during peeling and that the peel strength has little significance to the adhesion strength of the composite except when the latter is lower than the peel strength of rubber.

Smooth rubber failure

Compounds H and I bonded to metal experience almost smooth rubber failure. Here, the force-separation curve does not have

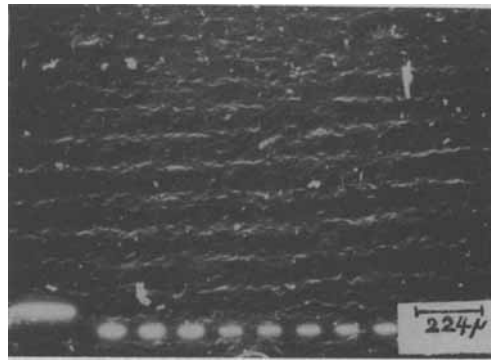

FIGURE 13 Fractograph of compound H showing the wavy pattern of the peeled metal surface (50×).

alternating maxima and minima as observed in stick-slip failure. In these cases, the rate of peeling is such that the force relaxation obtained while peeling is compensated by the force developed due to the pull of the rubber tab. The peel force values are given in Table II.

Figures 13 and 14 are the fractographs showing the failure surface of the metal part and Figures 15 and 16 are the fractographs showing the rubber part of the composite with compound H. In the case of Figure 15, no prominent and deep cracks are found. Moreover, the appearance of a close wavy pattern on the surface which is not very prominent implies that the failure, although

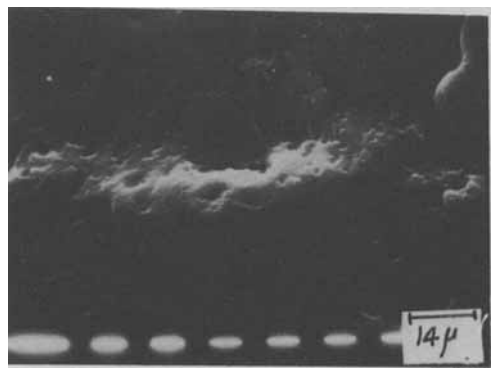

FIGURE 14 Fractograph showing the magnified view of the crest of a wave (800×).

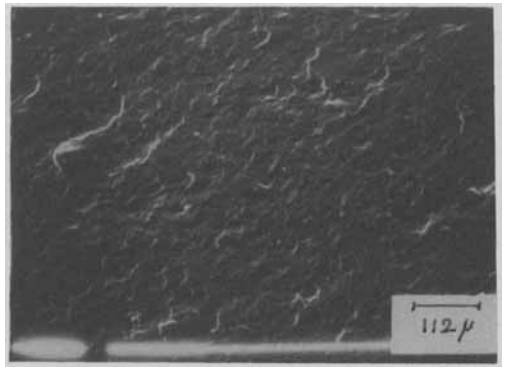

FIGURE 15 SEM photograph of compound H showing the peeled rubber surface (100×).

cohesive in rubber, occurred more easily and under less strain. The cohesive failure was confirmed by the swelling in benzene, as previously described. The magnified view of the crest of a wave shows dimples on the crest adjacent to a small crack (Figure 14). Low matrix strength of the rubber may be the reason for the smooth failure and low peel strength (Table II). Figure 15 shows the rubber fracture surface of the same composite. A magnified view of this surface (Figure 16) shows the hanging pattern of the waves throughout the matrix which may be due to the poor elastic recovery of the fracture surface.

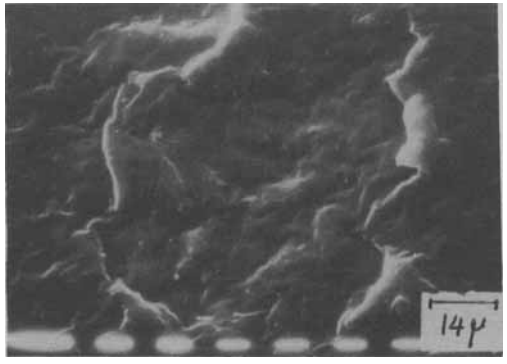

FIGURE 16 SEM photograph showing the magnified view of the peeled rubber surface. The hanging pattern of waves is clearly seen (compound H) (800×).

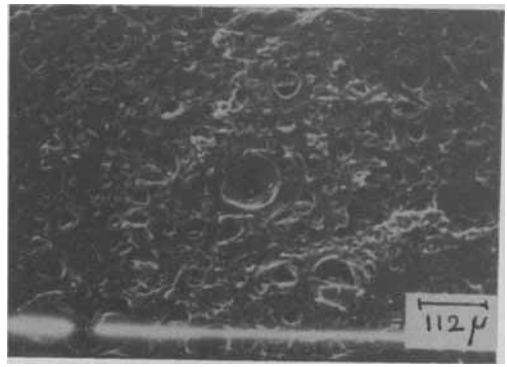

FIGURE 17 Photomicrograph of compound I showing the peeled metal surface (100×).

Figure 17 is the fractograph showing fractured metal surface of the composite corresponding to compound I containing 40 phr clay. This shows a large number of holes. These are the vacuoles caused by the dewetting of clay particles from the rubber matrix. A magnified view of a hole on the metal failure surface (Figure 18) shows that some of the holes are deep and the depth may be large enough to touch the adhesive surface. The locus of failure may have originated from the adhesive coated metal surface. A magnified view of a cavity on the rubber surface (Figure 19) shows the cavities are shallow and that there are small cracks on the sidewall of the

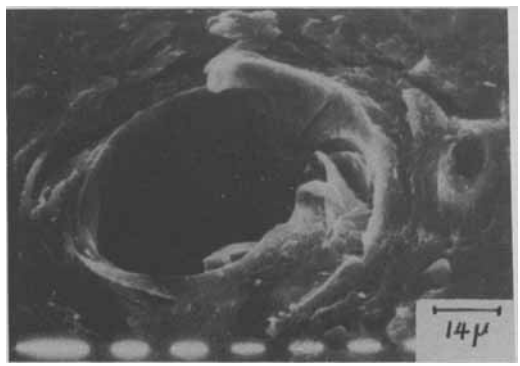

FIGURE 18 Photomicrograph showing the magnified view of a hole on the peeled metal surface (compound I) (800×).

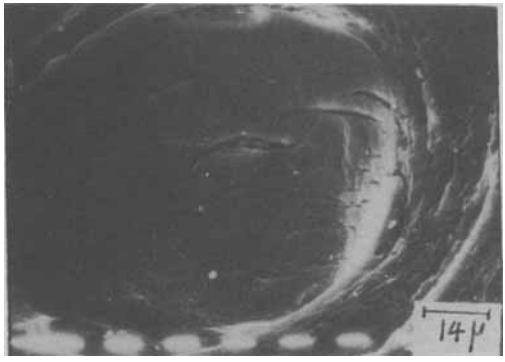

FIGURE 19 Fractograph showing the magnified view of a cavity on the peeled rubber surface (compound I) (800×).

cavities. These show that the adhesion between rubber and filler particle is poor which is further evidenced from the poor tear strength of the clay filled compounds as shown in Table III.

Intermittent rubber adhesive failure

In the case of silica-filled composites (Compounds F and G), a separate mode of failure was observed. The force-separation curve was not as smooth as was observed in the case of clay-filled or

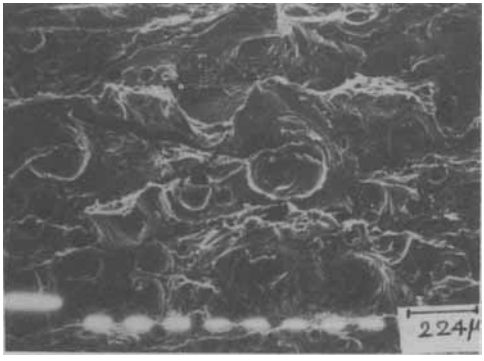

FIGURE 20 SEM photomicrograph of peeled metal surface of compound G (50×).

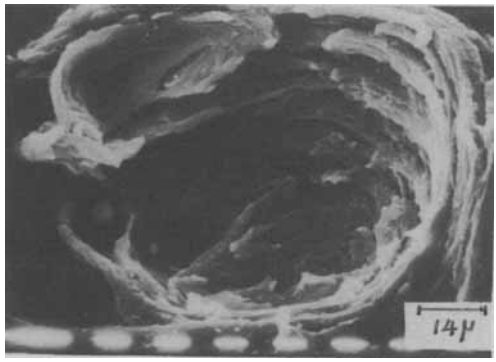

FIGURE 21 Photomicrograph showing the magnified view of a cavity on the peeled metal surface (compound G) (800×).

peroxide cured compounds and neither was the fracture surface. Since the silica-filled compound was white, tiny black spots observed on the failure surface of rubber show the adhesive failure.

The SEM fractograph of the typical failure surface (metal side) shows cup-shaped, shallow and deep cavities (Figure 20). This corresponds to the vaccuole formation due to the dewetting[14] of the silica filler from the rubber matrix. The magnified view (Figure 21) of the vaccuole shows a shattered cavity. The inside has systematic serration as if coiling of many layers of the matrix has taken place one over the other. During peeling, the matrix has undergone severe strain which is concentrated at different spots and the locus of failure begins from the centre of these spots, which later turn into cavities. Due to severe strain and multiple cracks, they give the coiling appearance. This is obviously different from the clay-filled compound showing the superior adhesion of silica filler to natural rubber. The tear strength of silica-filled compound is superior to the clay-filled compound as shown in Table III.

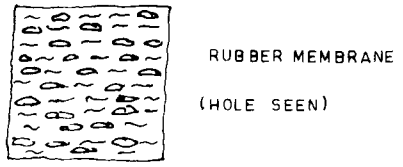

FIGURE 22 The thin swelled out layer of silica filled rubber compound. The holes seen correspond to the adhesive failure.

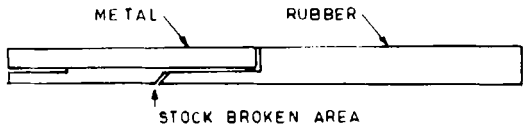

FIGURE 23 Figure showing the stock break.

When the failed metal strip was swollen in benzene, the white layer of rubber separated out. It looked like a net, having large number of holes in the membrane. This also shows the intermittent failure of the rubber and adhesive of the composite (Figure 22).

Breakage of rubber tab (stock break)

Rubber compounds A and B did not peel. Before peeling started, the tab was broken near the adhesive bonded region. The reason for the failure of the tab may be explained as follows. The compounds A and B have higher elongation at break as shown in Table III. Visual examination of the failure surface of the tab show a smooth curved tear face as given in Figure 23. Before peeling starts, the rubber tab elongates to a higher extent at the rate of 50 mm/min so that crystallization occurs at the peel front. This

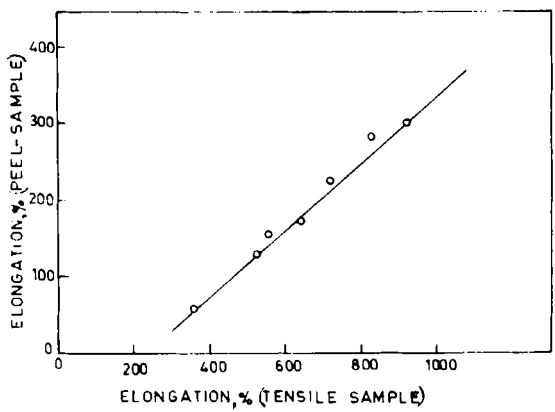

FIGURE 24 Percentage elongation of the tensile test specimen plotted against that of the peel test specimen for the same compound.

increases the resistance of the rubber compound to peel in a direction parallel to metal surface. So, once a crack is developed, it propagates in the direction of the weaker matrix and results in tab breakage.

On plotting per cent elongation at break against the percentage elongation of the peel test samples just before peel starts (Figure 24), it was observed that a linear relationship exists between the two. This implies that the 90° peel strength is dependent on the physical properties of the rubber vulcanizate when cohesive failure in rubber takes place.

CONCLUSIONS

The mechanism of failure of different rubber compounds in the 90° peel test for measuring the bond strength of rubber to metal *via* a widely used commercial adhesive was studied. It was found that:

(i) In stick-slip mode of failure, slow peeling occurs at the stick region which is responsible for the development of cracks on the failure surfaces.

(ii) When cohesive failure in rubber takes place, the peel strength is higher for the stick-slip mode of failure. Moreover, there exists a linear correlation between crosslink density and peel strength.

(iii) The minima values of the peel strength in the stick-slip mode of failure give a more consistent and reasonable value of failure strength of the composite than the maxima force values in the 90° peel test.

(iv) As compared to clay, silica filler-polymer interaction is higher. Dewetting of comparatively better bonded silica may be responsible for the mixed mode of failure in the silica-filled rubber-to-metal bonded composites.

Acknowledgement

This work was supported by the financial assistance from the Indian Council of Agricultural Research, New Delhi.

References

1. S. Buchan, *Rubber to Metal Bonding,* 2nd ed. (Crosby Lockwood, London, 1959).
2. G. W. Painter, *Adhesives Age* **3,** 36 (1960); *Rubber Age* **86,** 262 (1959).
3. J. Schultz and N. J. Westbrook, *J. Appl. Polym. Sci.* **21,** 2097 (1977).
4. B. Pickup and E. Weatherstone, *J. IRI,* **3,** 254 (1969).
5. D. W. Aubrey, G. N. Welding and T. Wong, *J. Appl. Polym. Sci.* **13,** 2193 (1969).
6. A. N. Gent, and G. R. Hamed, *Polym. Eng. Sci.* **17,** 462 (1977).
7. E. Cutts, *Developments in Adhesives 2,* A. J. Kinloch, Ed. (Applied Science Publishers, London, 1981).
8. K. J. Kim, C. J. Nelson, L. E. Vescelius and G. G. A. Bohm, *Scanning Electron Microscopy* **11,** 533 (1982).
9. L. Mullins, *J. Appl. Polym. Sci.* **2,** 1 (1959).
10. P. J. Flory and J. Rehner Jr., *J. Chem. Phys.* **11,** 521 (1943).
11. M. Porter, *Rubber Chem. Technol.* **40,** 866 (1967).
12. N. M. Mathew, A. K. Bhowmick and S. K. De, *ibid.* **55,** 51 (1982).
13. Pranab Kumar Pal, S. K. De, *J. Appl. Polym. Sci.* **28,** 659 (1983).
14. Pranab Kumar Pal, S. K. De, *Rubber Chem. Technol.* **55,** 1370 (1982).